RAD Conference Proceedings, vol. 6, pp. 110–118, 2022
ISSN 2466-4626 (online) | DOI: 10.21175/RadProc.2022.20
www.rad-proceedings.org

KINETIC STUDY OF THE OXIDATIVE DISSOLUTION OF URANIUM DIOXIDE AND TRIURANIUM OCTOXIDE IN CARBONATE MEDIA

N.M. Chervyakov[1,2], A.V. Boyarintsev[1,2*], I.A. Teplov[1,2], S.I. Stepanov[1,2]

[1]Ozersk Institute of Technology, Ozersk, Russia
[2]Mendeleev University of Chemical Technology, Moscow, Russia

Abstract. *The dissolution yield, reaction rate constant, and apparent activation energy values of oxidative dissolution of $UO_{2.25}$ and U_3O_8 (obtained in the temperature range 480°C–1200°C) powder samples in 1.0 mol/L $NaHCO_3$(Na_2CO_3) aqueous solutions at the fractional feeding mode of liquid hydrogen peroxide or crystalline sodium percarbonate ($2Na_2CO_3{\cdot}3H_2O_2$) at various temperatures are estimated, summarized and discussed. The conditions of powdered U_3O_8 samples for complete dissolution in carbonate systems have been defined. The obtained results are fundamental importance for the development and optimization of modes and conditions for alternative carbonate-based systems for voloxidized spent nuclear fuel oxidative dissolution.*

Key words: *uranium dioxide, triuranium octoxide, sodium carbonate, sodium bicarbonate, sodium percarbonate, hydrogen peroxide, oxidative dissolution, reaction rate constant, apparent activation energy.*

1. INTRODUCTION

Promising published results [1]–[8] on the applying of $M_2CO_3 - H_2O_2$ ($M = Na^+$ or NH_4^+) mixtures as dissolution systems led to the decision to use these media in new applications for the dissolution of various uranium-containing materials. The effectiveness of mixture $(NH_4)_2CO_3 - H_2O_2$ as a dissolvent medium has been demonstrated during for recovery of uranium from irradiated fuel [9], radioactive wastes [10,11], and metallic uranium [12]. The $Na_2CO_3 - H_2O_2$ mixture has been tested for leaching uranium from $(U,Gd)O_2$ nuclear fuel scrap [13] and uranium-bearing lime precipitate (sludge) [14,15].

Kinetic study of uranium oxides dissolution in carbonate media under oxidative conditions is critical for the development and improvement of a key stage in new alternative carbonate-based approaches for reprocessing spent nuclear fuel (SNF) [7]. At the same time, oxidation is the main way of dissolving UO_2-based SNF and U_3O_8-based voloxidized SNF in most applications of practical importance. The rate of uranium dioxide (UO_2) or triuranium octoxide (U_3O_8) oxidative dissolution is affected by the concentration and type(nature) of carbonate reagent, concentration of H_2O_2, temperature, and pH [3,4,8].

Casas et al. [16] determined the kinetic of UO_2 dissolution under oxidizing conditions, suggesting for the first time the mechanism of UO_2 oxidation-dissolution.

Three main sequential stages have been established for the process of UO_2 oxidative dissolution in aqueous carbonate solutions: (i) initial oxidation of UO_2 surface, (ii) coordination (binding) and complexation of U(VI) on the areas of the oxidized surface with HCO_3^-, CO_3^{2-} or OH^- ions, (iii) transfer from the surface into solution of the carbonate $[UO_2(CO_3)_3]^{4-}$ [17] and/or mixed uranyl(VI) peroxo-carbonate species $[UO_2(O_2)_x(CO_3)_y]^{(2-2x-2y)}$, where $x = 1–3$, $y = 3–x$ [3,4,18], with different solubility and stability in carbonate media.

It is generally considered that the second stage is a fast process compared to the oxidation of UO_2, and the latter should be considered as a slowest (rate-limiting) step of oxidative dissolution [19]. This is observed only for aqueous solutions with a high concentration of carbonate ions, when conditions are performed for the formation of stable soluble carbonate (in systems without free peroxide ion) and mixed uranyl(VI) peroxo-carbonate species.

The stage of UO_2 or U_3O_8 oxidation by H_2O_2 is necessary but insufficient condition for the dissolution of the oxide phase in the presence of H_2O_2. In the absence or in the presence of low concentrations of complexing ligands (HCO_3^-, CO_3^{2-} or OH^- ions) in the liquid phase, the oxidation/dissolution reaction slows down or stops completely. In this case, an oxidized layer is formed on the surface of UO_2 or U_3O_8 particles, and/or secondary U(VI)-containing poorly soluble phases that to form a precipitate. The formation of these secondary phases on the oxide surface reduces the surface area of the reaction, leads to blocking the accessible reactive surface of oxide for oxidizer and increases the diffusion resistance in a heterogeneous system. In a neutral non-complexing solution, dissolved UO_2^{2+} can pass into a corrosion product $UO_3{\cdot}xH_2O$ on an oxidized surface [20]. In the presence of H_2O_2, the composition of secondary precipitates depends on the concentration of H_2O_2, with schoepite ($(UO_2)_8O_2(OH)_{12}{\cdot}12H_2O$) dominating at lower concentrations ($\leq 10^{-4}$ mol/L) [21]. At high concentrations of H_2O_2, secondary peroxide uranyl(VI) phases are formed, such as studtite

*aboyarincev@muctr.ru

($[(UO_2)(O_2)(H_2O)_2]\cdot 2(H_2O)$) or metastudtite ($[(UO_2)(O_2)]\cdot 2(H_2O)$) [22]–[25]. As a rule, in such cases, structure development, crystal orientation and their morphology, uniformity and thickness of U(VI)-layer on the oxide surface depends on the concentration of H_2O_2 and determines the kinetic of oxidative dissolution process [26,27].

The rate of UO_2 and U_3O_8 dissolution increases with an increase in the CO_3^{2-} and HCO_3^- ions concentration, in the presence of which the formation of a layer of oxidation products is prevented and the surface of the reacting oxide particles remains free. However, in concentrated carbonate solution, a corrosion product UO_2CO_3 can be formed on the oxidized surface, which also blocks oxide dissolution [20].

Despite the data available in the scientific literature, additional more detailed studies are needed to study and understand the kinetic patterns of UO_2 and U_3O_8 with different physical properties dissolution in carbonate media. An actual task is to develop intensification methods to increase the dissolution rate of U_3O_8 powders as UO_2 volume oxidation (voloxidation) products. The voloxidation of SNF is aimed at the removal of volatile and gaseous fission products [7].

The study of the parameters of uranium oxides dissolution in basic media is fundamental scientific interest and has practical applications in the management of radioactive waste in the nuclear fuel cycle, including storage and reprocessing of SNF and radioactive waste.

The purpose of this article is to discuss and systematize obtained results of kinetic study of uranium dioxide and triuranium octoxide powders oxidative dissolution in aqueous solutions of sodium carbonates or bicarbonates in the presence of hydrogen peroxide. Additional purposes are the determination and comparison of the value of reaction rate constant in a wide range of temperature, concentration of reagents and other various conditions and procedures.

2. Materials and methods

Solid $NaHCO_3$, Na_2CO_3, $2Na_2CO_3\cdot 3H_2O_2$, Na_2O_2, ethylenediaminetetraacetic acid disodium salt, 8-oxyquinoline, and 30 % (9.8 mol/L) aqueous solution of H_2O_2 of the chemically pure grade were used.

Uranium dioxide powder as a starting material was used. The composition of the initial UO_2 powder, according to the X-ray diffraction (XRD) analysis corresponded to $UO_{2.25}$ (PDF–2/2010 № 20–1344). The specific surface area (*SSA*) value, calculated using the Brunauer, Emmett, and Teller (BET) method for the $UO_{2.25}$ powder sample was 3.3 m²/g. Powdered samples of U_3O_8, were obtained by heat treatment of the powdered $UO_{2.25}$ in the air atmosphere for 120 min in the calcinations temperature (t_C) range from 480°C to 1200°C. The heat treatment mode was as follows: 120 min of heating – 120 min of isothermal exposure – slow cooling together with the furnace. The heat treatment products were fine crystalline powders, whose colour, depending on the treatment temperature, ranged from olive green to black. In all cases, the final heat-treated product for $UO_{2.25}$ from 480 to 1200°C was U_3O_8 (PDF–2/2010 № 76–1850). Table 1 shows the *SSA* values for U_3O_8 powder samples.

Table 1. Data on the specific surface area of the U3O8 powder samples.

t_C, °C	480	600	800	1000	1200
SSA_{BET}, m²/g*	3.8	3.7	1.8	0.8	0.1

*SSA_{BET} – specific surface area (*SSA*) value, calculated using Brunauer, Emmett, and Teller (BET) method.

Figure 1 shows the micrographs for the UO_2 (1,2) and U_3O_8 (3–12) powder samples obtained with a scanning electron microscope (SEM).

An increase in the calcination temperature of the $UO_{2.25}$ initial powder leads to increasing the quantity of particle size fraction 10–40 μm and reducing the quantity of particle size fraction 1–6 μm for the U_3O_8 samples (see Table 2). Particle size distribution ($D50$) for $UO_{2.25}$ and U_3O_8 samples, obtained at 480, 600, 800, 1000, and 1200°C was 2.6, 5.8, 5.9, 8.6, 9.5, and 32.2 μm, respectively.

The process of $UO_{2.25}$ or U_3O_8 oxidative dissolution was carried out in 100 mL or 1000 mL jacketed stirred stainless steel reactor. The temperature was maintained with an accuracy of ±0.1°C. The mixing of the suspension was carried out with a magnetic stirrer.

In order to intensify and accelerate the oxidative dissolution, a horn type ultrasonic waveguide, connected to an ultrasonic wave generator and the console of the apparatus Bulava–P UZAP–3/22–OP (Center of Ultrasonic Technologies, Russia), was placed into the stainless steel reactor. The ultrasonic treatment during the dissolution was carried out at the frequency (υ) of 22±1.65 kHz and the intensity of (I) 10 W cm^{-2}.

The content of U(VI) in the aqueous solutions with concentration over 1.0 g/L was established by titration, using 8.4 mmol/L solution of ammonium vanadate as the titrant and diphenylamine-4-sulfonic acid sodium salt as the indicator [28]. The content of U(VI) in the solutions with concentration lower than 1.0 g/L was established by the spectrophotometric method with Arsenazo III (2,7-bis(2-arsonophenylazo)chromotropic acid) [29], per the absorbance spectra of the green-blue complex compound arsenazo-uranyl(VI) (λ_{max} = 651 nm, detection limit ~0.025–0.05 μgU/L) [30]. Before analysis, all liquid samples were centrifuged for 10 min at 1500 rpm.

The value of $UO_{2.25}$ or U_3O_8 dissolution yield (α) was calculated by the following equation: $\alpha = (M_\tau/M_i)\cdot 100$, where M_i is the initial quantity of the $UO_{2.25}(U_3O_8)$. The M_τ value was calculated based on the experimentally determined concentration of U(VI) in the liquid phase. The relative error in the determination of U(VI) concentration in alkaline solutions was 0.5 %.

Concentrations of H_2O_2 from were measured spectrophotometrically using UV–vis HP Diode Array Spectrophotometer 8452A with a one to 10 mm quartz cuvette at 350 nm [31] or titrimetrically [32].

The phase composition of $UO_{2.25}$ and U_3O_8 powders was determined by XRD [33]. Each sample was ground with an agate mortar. Diffraction patterns was recorded by mobile benchtop X-ray diffractometer D2 PHASER

(Bruker, Germany) using CuK_a radiation, Ni filter with a wavelength equal 1.54178 Å, and graphite monochromator. X-ray tube mode: (Cu) 10 mA, 30 kV. The diffraction patterns were collected at 25°C and over an angular range of 10 to 70° with a step size of 0.02° per step and a dwell time of 1.5 s per increment. Identification of diffraction patterns were performed using ICDD PDF–2 database and specialized software TOPAS/EVA.

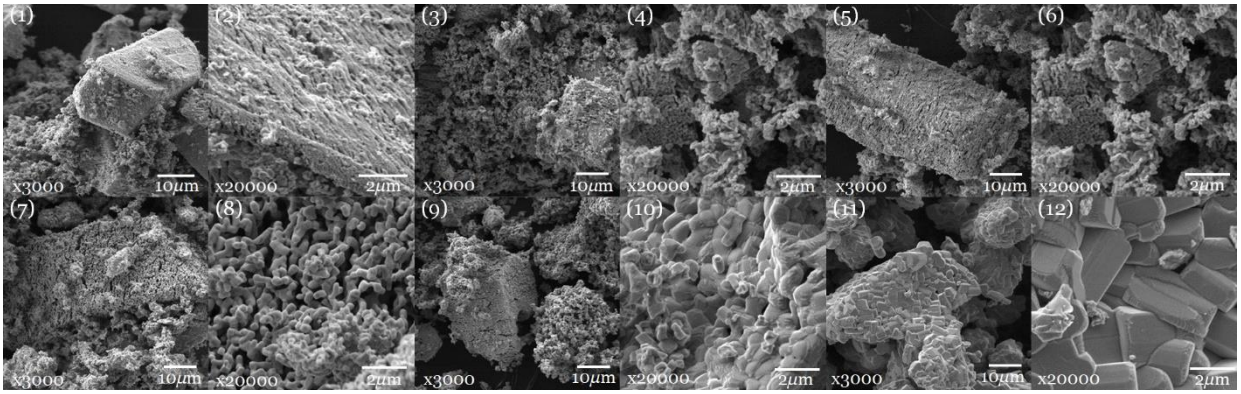

Figure 1. SEM micrographs of the initial UO_2 powdered sample (1,2) and U_3O_8 powdered samples, were obtained at 480°C (3,4), 600°C (5,6), 800°C (7,8), 1000°C (9,10), and 1200°C (11,12)

Table 2. Particle size distribution of $UO_{2.25}$ and U_3O_8 powder samples. Results from laser diffraction granulometry.

Size range, μm	Fraction (% by mass)					
	$UO_{2.25}$	U_3O_8(480°C)	U_3O_8(600°C)	U_3O_8(800°C)	U_3O_8(1000°C)	U_3O_8(1200°C)
1–2	35.31	22.78	24.93	19.68	14.27	2.39
2–3	20.67	10.59	10.40	9.15	9.04	1.72
3–4	11.22	6.53	5.78	5.19	6.16	1.49
4–5	6.77	5.38	4.25	3.89	4.80	1.62
5–6	6.76	5.62	5.28	4.54	3.63	1.57
6–7	2.90	4.06	4.17	3.28	3.04	1.72
7–8	1.87	3.55	3.02	2.53	3.57	1.60
8–9	4.48	4.17	3.12	3.04	3.85	1.51
9–10	5.63	4.56	3.83	3.42	3.35	1.41
10–20	4.40	25.83	27.21	18.04	19.09	13.23
20–30	0.00	6.92	8.02	27.19	29.03	16.39
30–40	0.00	0.00	0.00	0.05	0.16	12.27
40–50	0.00	0.00	0.00	0.00	0.00	40.97
50–60	0.00	0.00	0.00	0.00	0.00	2.10
Total	100.00	100.00	100.00	100.00	100.00	100.00

The morphology of the initial samples of uranium oxide powders was studied using Vega3 scanning (raster) electron microscope (Tescan, Czech Republic) with lanthanum hexaboride (LaB_6) cathode and in high vacuum mode. A thin layer of carbon (up to 15 nm) was previously sprayed onto the sample to create a conductive coating. The survey was carried out using the Everhart–Thornley detector for secondary electrons at an accelerating voltage equal 5 kV.

The specific surface area was calculated by the BET [34] method using QuadraWin software (version 5.02) based on a nitrogen adsorption/desorption isotherms at –196°C on a Quadrasorb Kr/SI system (Quantachrome Instruments, USA). The samples were outgassed at 80°C overnight before analysis was performed. Nitrogen was used as the adsorbate gas, and the BET isotherm was determined with the ratio of the gas pressure to the saturated vapour pressure $z = P / P_0$ ranging from 0.1 to 0.35.

The particle size distribution was measured by laser diffraction granulometry. To determine granulometric composition of powders, NanoTec Laser Particle Sizer Analysette 22 (Fritsch, Germany) was used. The range of measurable particle sizes is from 10 nm to 2000 μm. To ensure maximum resolution, measurements were performed with seven positions of measuring cell during dispersion of studied sample in water medium with exposure to ultrasound with the frequency of 36 kHz and with the power of 70 W. Particle distribution per sizes was calculated with the usage of a specialized software by an algorithm based on the Fraunhofer diffraction theory (lower boundary of particle sizes: 100 nm).

To determine the dissolution rate constants and the rate-limiting stage of process, mathematical modeling of the experimentally obtained dependences $\alpha = f(\tau)$ with applying of fourteen kinetic models was carried out [8]. The results of the mathematical modeling showed that the Yander equation [35] satisfactorily describes experimental kinetic curves and can be used to calculation of oxidative dissolution rate constant (k) [36] for all studied bicarbonate/carbonate-peroxide system under various conditions. The values of k were determined by the slope values of linear anamorphoses (characterized by the correlation coefficient (R) value)

in the coordinates of the Yander equation, which corresponded to the initial ascending branch of the kinetic curve (from zero to 60 min of agitation).

Based on the slope value of the line dependence in the coordinates ln$k$ – 1/T, the value of the apparent activation energy (E_{app}) of the UO_2 and U_3O_8 powder samples oxidative dissolution process in all studied systems was calculated.

3. Results and discussion

A necessary condition for UO_2 and U_3O_8 dissolution in M_2CO_3 solutions, where M is an alkali metal or ammonium cation, is to achieve and maintain the required oxidation-reduction potential (ORP) value in the system. Hydrogen peroxide is a salt-free reagent and has a suitable ORP that can oxidize U(IV), U(V) and exhibits the highest rate of uranium oxidation. The role of H_2O_2 in dissolution processes is not limited only to oxidation, because the peroxide anion takes an active part in the formation of highly soluble uranyl(VI) peroxo-carbonate anionic species [3,4,18]. Therefore, according to some authors [3]–[13], H_2O_2 is the most suitable oxidizer for the processes of UO_2 and U_3O_8 oxidative dissolution in carbonate/bicarbonate media.

The option of single addition of H_2O_2 entire amount to the carbonate solution before agitation starting as a rule, it does not allow achieving complete dissolution of U_3O_8. To maintain a constant value of ORP in the carbonate oxidizing system, it is necessary to carry out fractional feeding of H_2O_2 aqueous solution [8] or crystalline sodium percarbonate ($2Na_2CO_3{\cdot}3H_2O_2$) or sodium peroxide (Na_2O_2) which are considered as alternative peroxide oxidants in carbonate-based dissolving systems. This is most relevant for the dissolution of highly calcined well-crystallized U_3O_8 samples with a low specific surface area, whose dissolution rate in carbonate solutions is low, while free H_2O_2, depending on concentration of carbonate and temperature completely decomposes after 10–20 min.

The physical characteristics (morphology, specific surface area, particle size distribution) of UO_2 and U_3O_8 powder are important factors affecting on the dissolution rate. The temperature regime of UO_2 voloxidation affects on the physical characteristics of the resulting product (U_3O_8). Consequently, voloxidized SNF powders with different characteristics can be supplied to the oxidative dissolution stage. Their dissolution rate in the carbonate-peroxide system will be different.

It is known that amorphous UO_2 is more susceptible to chemical action and oxidation and is more soluble than crystalline UO_2 [37,38]. Additional grinding of UO_2 or U_3O_8 samples before dissolution contributes to a sharp increase in the dissolution rate. However, the grinding stage in the industrial scale of SNF reprocessing is unacceptable due to air pollution with radioactive particles.

In the process of voloxidation, the crystal lattice of UO_2 is rearranged. As a result, compact UO_2 turns into powdered U_3O_8. Therefore, the powdered fuel composition is supplied to the oxidative leaching step.

However, it should be noted that studying the behavior of uranium dioxide during oxidative dissolution in carbonate-peroxide systems may be also relevant, for example, in the case of investigation the processes of SNF corrosion under long-term disposal in geological repositories or developing processes for uranium leaching from technogenic and mineral raw materials.

A key task for the development of alternative oxidative carbonate systems is to study the effect of various parameters on the kinetic of dissolution/leaching of uranium oxides. Such parameters may include: (i) physical characteristics of uranium oxide, (ii) nature and concentration of the carbonate reagent and oxidizer/complexing reagent, (iii) pH value, (iv) ORP value, (v) temperature, (vi) agitation time, (vii) process mode, and etc. In addition, it is important to determine the conditions for intensification and increasing the rate of oxidative dissolution of uranium oxides in carbonate media, as well as obtaining concentrated U(VI)-containing carbonate solutions.

In this work, special focus was paid to the study of the impact of the physical properties of U_3O_8 powder and temperature on the rate of oxidative dissolution of UO_2 and U_3O_8 in $NaHCO_3$(Na_2CO_3) – H_2O_2 systems. The impact of these parameters is still not sufficiently studied and described in the literature. To compare, systematize and evaluate the results obtained, other conditions and systems are also selectively considered.

In the process of powdered $UO_{2.25}$ sample oxidative dissolution, an increase in the concentration of H_2O_2 from 0.1 to 0.9 mol/L in 1.0 mol/L Na_2CO_3 solution leads to an increase in the dissolution rate and $UO_{2.25}$ dissolution yield value (Table 3). The k value increases more than twice, from $3{\cdot}10^{-4}$ to $7{\cdot}10^{-4}$ min^{-1}. Table 3 shows the maximum α value achieved during agitation time equal τ.

In the case of powdered $UO_{2.25}$ dissolution in 1.0 mol/L $NaHCO_3$ – 0.1 mol/L H_2O_2 mixture with fractional feeding of liquid H_2O_2 or in the case of fractional feeding of crystalline $2Na_2CO_3{\cdot}3H_2O_2$ into aqueous solution, an increase in temperature from 25 to 75°C leads to an increase in the k value by 3–4 times and α value by 15–20% (Table 3). The feeding mode of crystalline $2Na_2CO_3{\cdot}3H_2O_2$ into the aqueous solution was such that, with the addition of the full amount of percarbonate, the concentration of carbonate ions in the final aqueous solution was 1.0 mol/L [8]. Sodium percarbonate rapidly dissolves in water and dissociates into Na^+ ions, CO_3^{2-} ions, and H_2O_2:

$$2Na_2CO_3{\cdot}3H_2O_2 \rightarrow 4Na^+ + 2CO_3^{2-} + 3H_2O_2 \quad (1)$$

As shown earlier [8], an increasing in the calcinations temperature of U3O8 powder from 480 to 1200°C leads to decreasing of the sample dissolution rate in aqueous 1.0 mol/L Na2CO3 – 0.1 mol/L H2O2 solutions with fractional feeding of H2O2 every 10 min. The k value is reduced by two orders of magnitude. This is caused by a decrease in a SSA value and an increase in the average particle size of U3O8 sample. Complete dissolution at 75°C for 90 min was achieved only for the U3O8 sample obtained at 480°C [8].

With an increase in temperature from 25 to 75°C in 1.0 mol/L Na2CO3 – 0.1 mol/L H2O2 system, the α value increased from 34.5% to more than 99.9% for the U3O8(600°C) sample. In the case of U3O8(1200°C)

sample the increase of α occurred only with an increase in temperature to 50°C (41.5%) and then did not depend on temperature (Table 4).

An increase in the H2O2 concentration from 0.1 to 0.5 mol/L when U3O8(1200°C) powder dissolution in 1.0 mol/L Na2CO3 solution led to an increase in k by 2–3 times, and the α value increased from 43 to 86% for 240 min of agitation (Table 4). An increase of Na2CO3 concentration has significant effect on the U3O8 powders dissolution rate. The k value increases in 5–8 times with an increase in the Na2CO3 concentration from 0.5 to 2.0 mol/L (75 °C). At the same time, the α(U3O8(1200°C) value increases to 90% in 240 min of agitation.

Table 3. The *k* values [36] for the oxidative dissolution of powdered UO_2 in 1.0 mol/L $NaHCO_3$(Na_2CO_3) – 0.1–0.9 mol/L H_2O_2 solutions, calculated in the coordinates of the Yander equation [35]. Liquid -to-solid ratio (L/S) = 50/1. *t* – the temperature of dissolution; *k* – the calculated value of rate constant of oxidative dissolution; *R* – the correlation coefficient; *τ* – the agitation time; *α* – the dissolution yield value for UO_2 powdered sample.

Dissolution media	Oxidizer	*t*, °C	*k*, min^{-1}	*R*	*τ*, min	*α*, %
1.0 mol/L Na_2CO_3	0.1 mol/L H_2O_2	75	$3\cdot10^{-4}$	0.9119	60	33.2
	0.2 mol/L H_2O_2		$4\cdot10^{-4}$	0.9545	50	35.0
	0.5 mol/L H_2O_2		$4\cdot10^{-4}$	0.9315		38.0
	0.9 mol/L H_2O_2		$7\cdot10^{-4}$	0.9434	60	45.0
1.0 mol/L $NaHCO_3$	0.1 mol/L H_2O_2	25	$1.2\cdot10^{-3}$	0.9879	90	62.6
		40	$1.6\cdot10^{-3}$	0.9535		66.3
		50	$2.1\cdot10^{-3}$	0.9403	120	70.0
		60	$2.6\cdot10^{-3}$	0.9505	90	74.7
		75	$3.1\cdot10^{-3}$	0.9792	60	80.0
$2Na_2CO_3\cdot3H_2O_2$ (1.0 mol/L Na_2CO_3)		25	$3\cdot10^{-4}$	0.9466	210	77.9
		50	$8\cdot10^{-4}$	0.9037	180	87.3
		75	$1.4\cdot10^{-3}$	0.8852		96.4

When using of Na_2O_2 as oxidizer, the U_3O_8(1200°C) dissolution yield value doesn't exceed 15% (see Table 4). The low solubility of U_3O_8 in the presence of Na_2O_2 is associated with an increase in the pH of the carbonate solution (>12) as a result of Na_2O_2 decomposition with the formation and accumulation (at fractional feeding mode of an oxidizing agent) of sodium hydroxide (NaOH). When Na_2O_2 comes in contact with water, it gets hydrolyzed to form NaOH and H_2O_2 as follows:

$$Na_2O_2 + 2H_2O \rightarrow 2NaOH + H_2O_2 \quad (2)$$

Under such conditions, alkaline hydrolysis of soluble carbonate and mixed peroxo-carbonate species of U(VI) occurs to form poorly soluble sodium polyuranates [8].

In 1.0 mol/L $NaHCO_3$ – 0.1 mol/L H_2O_2 system, the completeness of U_3O_8(480°C), U_3O_8(600°C), and U_3O_8(800°C) powder dissolution was achieved only at 75°C for 30 min, 90 min, and 180 min of agitation, respectively. Under these conditions, the *α* maximum value for U_3O_8(1200°C) powder sample during 240 min of agitation did not exceed 70% (Table 5).

An increase in temperature from 25 to 75°C in the bicarbonate system allowed to increase *α* values for U_3O_8(480°C), U_3O_8(600°C), and U_3O_8(800°C) samples, from 47.2%, 34.2%, and 31.9%, respectively, to more than 99.9%, and for the U_3O_8(1200°C) sample from 8.0 to 66.9% (Table 5).

Thus, samples of U_3O_8 powder obtained in the temperature range of 480–800°C can be relatively quickly and quantitatively dissolved in 1.0 mol/L $NaHCO_3$(Na_2CO_3) – *x* mol/L H_2O_2 (*x* = 0.1–0.5) systems. However, the dissolution rate of U_3O_8 samples obtained at temperatures above 1000°C is significantly slowed down, and as a result, the completeness of their dissolution is not achieved even for continuous long-term agitation and at increased consumption (concentration) of H_2O_2. Chemical and mechanical (ultrasonication) methods can be used to intensify the process of UO_2 and U_3O_8 oxidative dissolution [39,40]. Chemical intensification consists in the addition of compounds that form highly soluble stable species with uranyl(VI)-ion. As such reagents, for example, the ethylenediaminetetraacetic acid disodium salt (Trilon B) and 8-oxyquinoline (8-Ox) can be used.

When the U_3O_8(1200°C) powder is dissolved, the *k* value with addition of 0.1 mol/L 8-Ox in the 1.0 mol/L Na_2CO_3 – 0.1 mol/L H_2O_2 system increases three times (from $7.7\cdot10^{-5}$ to $2.5\cdot10^{-4}$ min^{-1}) at 50°C and twenty times (from $6.1\cdot10^{-5}$ to $1.2\cdot10^{-3}$ min^{-1}) once at 75°C. When 0.1 mol/L Trilon B is added to the system, the *k* value increases twenty times (from $7.7\cdot10^{-5}$ to $1.5\cdot10^{-3}$ min^{-1}) at 50°C and forty times (from $6.1\cdot10^{-5}$ to $2.4\cdot10^{-3}$ min^{-1}) at 75°C. At the same time, the *α*(U_3O_8(1200°C)) value increases from 42.7 to 90% in the case of 0.1 mol/L 8-Ox and to >99.9% in the case of 0.1 mol/L Trilon B (at 75°C).

Ultrasonication of U_3O_8(800°C) powder suspension in 1.0 mol/L Na_2CO_3 – 0.1 mol/L H_2O_2 solution makes it possible to significantly increase the oxidative dissolution rate and generating concentrated U(VI)-containing carbonate solutions (>150 gU(VI)/L) with a decrease L/S from 50/1 to 3–5/1 [34].

However, in this case, it seems that an adjustment of the pH of the carbonate solution is required (for example, a limited supply of gaseous CO_2 to the suspension layer [34]) to prevent the formation of less soluble U(VI) compounds due to the accumulation of alkali, which is formed during the dissolution of UO_2 and U_3O_8. While at low yield and concentration of U(VI) into carbonate solution, the pH changes during oxidative dissolution are insignificant, since the solution is strongly buffered with HCO_3^- or/and CO_3^{2-} ions.

Table 4. The *k* values [36] for the oxidative dissolution of powdered U_3O_8 samples in carbonate-peroxide solutions, calculated in the coordinates of the Yander equation [35]. L/S = 50/1.

Oxide powder	Dissolution media	Oxidizer	*t*, °C	*k*, min^{-1}	*R*	*τ*, min	*α*, %
U_3O_8(480°C)	0.5 mol/L Na_2CO_3	0.1 mol/L H_2O_2	25	$3\cdot10^{-4}$	0.9382	180	85.1
			50	$1.8\cdot10^{-3}$	0.9577		88.1
			75	$7.1\cdot10^{-3}$	0.8810		98.9
	1.0 mol/L Na_2CO_3		25	$3.8\cdot10^{-4}$	0.9602		88.1
			50	$2.1\cdot10^{-3}$	0.9488		91.6
			75	$2.3\cdot10^{-2}$	0.9644	90	>99.9
	1.5 mol/L Na_2CO_3		25	$4.8\cdot10^{-4}$	0.9576	180	91.1
			50	$2.6\cdot10^{-3}$	0.9463		95.6
			75	$1.5\cdot10^{-2}$	0.9966	60	>99.9
	2.0 mol/L Na_2CO_3		25	$5.7\cdot10^{-4}$	0.9710	180	95.6
			50	$4.8\cdot10^{-3}$	0.9786		>99.9
			75	$1.9\cdot10^{-2}$	0.9332	30	
U_3O_8(600°C)	1.0 mol/L Na_2CO_3		25	$2\cdot10^{-4}$	0.9738	300	34.5
			40	$8\cdot10^{-4}$	0.9199		66.4
			50	$2.1\cdot10^{-3}$	0.9686		98.3
			60	$3.9\cdot10^{-3}$	0.9554		99.2
			75	$7.0\cdot10^{-3}$	0.9783	90	>99.9
U_3O_8(800°C)	0.5 mol/L Na_2CO_3		25	$2.2\cdot10^{-4}$	0.8948	180	74.0
			50	$1.3\cdot10^{-3}$	0.9333		76.6
			75	$5.2\cdot10^{-3}$	0.9536		93.8
	1.0 mol/L Na_2CO_3		25	$2.8\cdot10^{-4}$	0.9677		76.6
			50	$1.4\cdot10^{-3}$	0.9162		79.7
			75	$4.0\cdot10^{-3}$	0.9794	120	89.0
	1.5 mol/L Na_2CO_3		25	$3.5\cdot10^{-4}$	0.9646	180	79.2
			50	$1.8\cdot10^{-3}$	0.9023		83.1
			75	$1.4\cdot10^{-2}$	0.9368	60	>99.9
	2.0 mol/L Na_2CO_3		25	$4.2\cdot10^{-4}$	0.9769	180	83.1
			50	$3.0\cdot10^{-3}$	0.9396		86.9
			75	$1.5\cdot10^{-2}$	0.9726	60	>99.9
U_3O_8(1000°C)	1.0 mol/L Na_2CO_3		75	$2\cdot10^{-3}$	0.9895	300	67.2
U_3O_8(1200°C)	0.5 mol/L Na_2CO_3		25	$1.3\cdot10^{-5}$	0.9332	180	17.7
			50	$5.7\cdot10^{-5}$	0.9295		31.7
			75	$1.4\cdot10^{-4}$	0.9941		42.1
	1.0 mol/L Na_2CO_3		25	$2.0\cdot10^{-5}$	0.9912		18.2
			50	$1.1\cdot10^{-4}$	0.9838		36.9
			75	$2.1\cdot10^{-4}$	0.9599		58.0
	1.5 mol/L Na_2CO_3		25	$2.2\cdot10^{-5}$	0.8712		20.0
			50	$9.8\cdot10^{-5}$	0.8630		40.0
			75	$4.5\cdot10^{-4}$	0.9134		80.1
	2.0 mol/L Na_2CO_3		25	$2.3\cdot10^{-5}$	0.9079		21.6
			50	$1.0\cdot10^{-4}$	0.9002		43.1
			75	$5.9\cdot10^{-4}$	0.9591		91.0
U_3O_8(1200°C)	1.0 mol/L Na_2CO_3	0.2 mol/L H_2O_2	75	$1\cdot10^{-4}$	0.9596	240	62.3
		0.5 mol/L H_2O_2	75	$1.6\cdot10^{-4}$	0.9510		86.0
U_3O_8(480°C)	$2Na_2CO_3\cdot3H_2O_2$ (1.0 mol/L Na_2CO_3)		25	$4\cdot10^{-4}$	0.9221	210	96.4
			40	$9\cdot10^{-4}$	0.9456	180	93.9
			50	$1.7\cdot10^{-3}$	0.9532	120	92.4
			60	$3.7\cdot10^{-3}$	0.9437	120	99.2
			75	$1.7\cdot10^{-2}$	0.8022	60	>99.9
U_3O_8(1200°C)			25	$6\cdot10^{-6}$	0.9139	270	38.0
			40	$3.6\cdot10^{-5}$	0.9385	210	35.4
			50	$3.9\cdot10^{-5}$	0.9354	270	69.7
			60	$4.4\cdot10^{-5}$	0.9406	210	75.2
			75	$4.2\cdot10^{-4}$	0.9180	150	99.7
U_3O_8(1200°C)	1.0 mol/L Na_2CO_3	0.1 mol/L Na_2O_2		$1.5\cdot10^{-5}$	0.9474	180	14.7

Table 5. The *k* values [36] for the oxidative dissolution of powdered U_3O_8 samples in 1.0 mol/L $NaHCO_3$ – 0.1 mol/L H_2O_2 solutions, calculated in the coordinates of the Yander equation [35]. L/S = 50/1.

Oxide powder	*t*, °C	*k*, min^{-1}	*R*	*τ*, min	*α*, %
U_3O_8(480°C)	25	$3\cdot10^{-4}$	0.9901	210	47.2
	40	$7\cdot10^{-4}$	0.9741	210	61.9
	50	$1.1\cdot10^{-3}$	0.9479	150	76.7
	60	$3.2\cdot10^{-3}$	0.9663	60	79.5
	75	$2.2\cdot10^{-2}$	0.9437	30	>99.9
U_3O_8(600°C)	25	$2\cdot10^{-4}$	0.9283	180	34.2
	40	$5\cdot10^{-4}$	0.9781	240	64.1
	50	$1\cdot10^{-3}$	0.9899	180	93.3
	60	$2.2\cdot10^{-3}$	0.9864	150	94.0
	75	$6.1\cdot10^{-3}$	0.9750	90	>99.9
U_3O_8(800°C)	25	$5\cdot10^{-5}$	0.9125	240	31.9
	40	$1\cdot10^{-4}$	0.9956		62.1
	50	$2\cdot10^{-4}$	0.9823		92.3
	60	$1.3\cdot10^{-3}$	0.9905		95.9
	75	$4.5\cdot10^{-3}$	0.9623	180	>99.9
U_3O_8(1000°C)	25	$2\cdot10^{-5}$	0.9829	210	29.1
	40	$7\cdot10^{-5}$	0.9699		56.8
	50	$2\cdot10^{-4}$	0.9294		79.0
	60	$6.0\cdot10^{-4}$	0.9594		87.7
	75	$1.8\cdot10^{-3}$	0.9590		91.2
U_3O_8(1200°C)	25	$1\cdot10^{-6}$	0.8945		8.0
	40	$2\cdot10^{-6}$	0.8959		10.5
	50	$3\cdot10^{-6}$	0.9432		12.9
	60	$2.7\cdot10^{-5}$	0.9464		39.9
	75	$8.1\cdot10^{-5}$	0.9442		66.9

Table 6. The apparent activation energy (E_{app}) values for the oxidative dissolution of powdered UO_2 and U_3O_8 samples in carbonate/bicarbonate – peroxide solutions.

Powder sample	Dissolution media	Oxidizer	E_{app}, kJ/mol
$UO_{2.25}$	1.0 mol/L $NaHCO_3$	0.1 mol/L H_2O_2	16.8
U_3O_8(480°C)			72.0
U_3O_8(600°C)			59.5
U_3O_8(800°C)			81.4
U_3O_8(1000°C)			79.7
U_3O_8(1200°C)			79.1
$UO_{2.25}$	$2Na_2CO_3\cdot3H_2O_2$ (1.0 mol/L Na_2CO_3)		26.7
U_3O_8(480°C)			59.7
U_3O_8(1200°C)			63.1
U_3O_8(480°C)	0.5 mol/L Na_2CO_3	0.1 mol/L H_2O_2	54.6
U_3O_8(800°C)			54.4
U_3O_8(1200°C)			41.2
U_3O_8(480°C)	1.0 mol/L Na_2CO_3		60.2
U_3O_8(600°C)			65.1
U_3O_8(800°C)			52.5
U_3O_8(1200°C)			40.9
U_3O_8(480°C)	1.5 mol/L Na_2CO_3		59.7
U_3O_8(800°C)			64.2
U_3O_8(1200°C)			52.0
U_3O_8(480°C)	2.0 mol/L Na_2CO_3		60.6
U_3O_8(800°C)			61.2
U_3O_8(1200°C)			55.8

The E_{app} value [35] in the case of $UO_{2.25}$ powder dissolution in 1.0 mol/L $NaHCO_3$ – 0.1 mol/L H_2O_2 was 16.8 kJ/mol and 26.7 kJ/mol with fractional feeding of $2Na_2CO_3\cdot3H_2O_2$ into aqueous suspension (Table 6). Estimated E_{app} values indicate, that the $UO_{2.25}$ oxidative dissolution process occurs in the external diffusion region.

The E_{app} values for the U_3O_8 powder oxidative dissolution process in carbonate media vary in the range from 40.9 to 81.4 kJ/mol. In all cases, the E_{app} calculated value is more than 40 kJ/mol, which indicates that the process is taking place in the kinetic region. Thus, in the region of high concentrations of $NaHCO_3$ and Na_2CO_3, the U_3O_8 powder oxidative

dissolution total process rate is limited by the rate of the chemical reaction of oxide surface oxidation. At the same time, the oxidation rate depends on the oxidant (H_2O_2) concentration and oxide particles surface characteristics.

4. Conclusion

The kinetic data of the oxidative dissolution of UO_2 and U_3O_8 powder samples in 1.0 mol/L $NaHCO_3$ and 0.5–2.0 mol/L Na_2CO_3 aqueous solutions at the fractional feeding mode of the hydrogen peroxide at various temperatures are summarized and discussed in the article.

The possibility of applying of sodium percarbonate as an alternative combined oxidizing and carbonate reagent for dissolving $UO_{2.25}$ and U_3O_8 powders is shown.

The conditions for complete dissolution of powdered U_3O_8 samples obtained at temperatures of 480–1200°C in systems of 1.0 mol/L $NaHCO_3$(0.5–2.0 mol/L Na_2CO_3) – 0.1–0.5 mol/L H_2O_2 have been established.

The dissolution of U_3O_8 powder samples obtained at temperatures above 1000°C requires intensification due to the addition of a complexing agent or ultrasonic treatment.

The obtained data can be useful in the development modes and conditions for alternative carbonate-based systems for oxidative dissolution of voloxidized spent nuclear fuel.

Acknowledgements: *The work was carried out with the financial support of the Russian Science Foundation. Grant number 20-63-46006.*

References

1. J. B. Hiskey, “Hydrogen peroxide leaching of uranium in carbonate solutions,” *Trans. Instn. Min. Met.*, vol. 89, pp. C145–C152, 1980.
2. N. Asanuma et al., “Anodic dissolution of UO_2 pellet containing simulated fission products in ammonium carbonate solution,” *J. Nucl. Sci. Technol.*, vol. 43, no. 3, pp. 255–262, 2006. https://doi.org/10.1080/18811248.2006.9711087
3. S. M. Peper et al., “Kinetic study of the oxidative dissolution of UO_2 in aqueous carbonate media,” *Ind. Eng. Chem. Res.*, vol. 43, no. 26, pp. 8188–8193, 2004. https://doi.org/10.1021/ie049457y
4. S. C. Smith, S. M. Peper, M. Douglas, K. L. Ziegelgruber, E. C. Finn, “Dissolution of uranium oxides under alkaline oxidizing conditions,” *J. Radioanal. Nucl. Chem.*, vol. 282, pp. 617–621, 2009. https://doi.org/10.1007/s10967-009-0182-8
5. D. Y. Chung et al., “Oxidative leaching of uranium from SIMFUEL using Na_2CO_3–H_2O_2 solution,” *J. Radioanal. Nucl. Chem.*, vol. 284, pp. 123–129, 2010. https://doi.org/10.1007/s10967-009-0443-6
6. S. I. Stepanov, A. V. Boyarintsev, A. M. Chekmarev, “Physicochemical foundations of spent nuclear fuel leaching in carbonate solutions,” *Dokl. Chem.*, vol. 427, pp. 202–206, 2009. https://doi.org/10.1134/S0012500809080060
7. S. I. Stepanov, A. V. Boyarintsev, “Reprocessing of spent nuclear fuel in carbonate media: Problems, achievements, and prospects,” *Nucl. Eng. Technol.*, vol. 54, no. 7, pp. 2339–2358, 2022. https://doi.org/10.1016/j.net.2022.01.009
8. N. M. Chervyakov, A. V. Boyarintsev, A. V. Andreev, S. I. Stepanov, “Oxidative dissolution of triuranium octoxide in carbonate solutions,” in *Proc. 9th Int. Conf. on Radiation in Various Fields of Research (RAD 2021)*, Herceg Novi, Montenegro, 2021, pp. 68–74. https://doi.org/10.21175/RadProc.2021.13
9. C. Z. Soderquist et al., “Dissolution of irradiated commercial UO_2 fuels in ammonium carbonate and hydrogen peroxide,” *Ind. Eng. Chem. Res.*, vol. 50, no. 4, pp. 1813–1818, 2011. https://doi.org/10.1021/ie101386n
10. B. Kweto, D. R. Groot, E. Stassen, J. Suthiram, J. R. Zeevaart, “Kinetic study of uranium residue dissolution in ammonium carbonate media,” *J. Radioanal. Nucl. Chem.*, vol. 302, pp. 131–137, 2014. https://doi.org/10.1007/s10967-014-3396-3
11. L. Stassen, J. Suthiram, “Initial development of an alkaline process for recovery of uranium from ^{99}Mo production process waste residue,” *J. Radioanal. Nucl. Chem.*, vol. 305, pp. 41–50, 2015. https://doi.org/10.1007/s10967-015-3974-z
12. C. Z. Soderquist, B. K. McNamara, B. Oliver, “Dissolution of uranium metal without hydride formation or hydrogen gas generation,” *J. Nucl. Mater.*, vol. 378, no. 3, pp. 299–304, 2008. https://doi.org/10.1016/j.jnucmat.2008.05.014
13. K. W. Kim et al., “Recovery of uranium from (U,Gd)O_2 nuclear fuel scrap using dissolution and precipitation in carbonate media,” *J. Nucl. Mater.*, vol. 418, no. 1–3, pp. 93–97, 2011. https://doi.org/10.1016/j.jnucmat.2011.06.019
14. 이일희, 이근영, 정동용, 김광욱, 이근우, 문제권, "우라늄 함유 석회침전물의 용해 및 침전에 의한 U 제거," 한국방사성폐기물학회지, 10권 2호, 77~85쪽, 2012.
(E. H. Lee, K. Y. Lee, D. Y. Chung, K. W. Lee, J. K. Moon, “Removal of uranium from U-bearing lime-precipitate using dissolution and precipitation methods,” *J. Korean Radioact. Waste Soc.*, vol. 10, no. 2, pp. 77–85, 2012.) https://doi.org/10.7733/jkrws.2012.10.2.077
15. 이일희, 양한범, 이근영, 김광욱, 정동용, 문제권, "알카리화 및 산성화에 의한 우라늄 함유 슬러지의 열분해 고체 폐기물로부터 우라늄 제거," 한국방사성폐기물학회지, 11권 2호, 85~93쪽, 2013.
E. H. Lee et al., “Removal of uranium by an alkalization and an acidification from the thermal decomposed solid waste of uranium-bearing sludge,” *J. Korean Radioact. Waste Soc.*, vol. 11, no. 2, pp. 85–93, 2013. http://doi.org/10.7733/jkrws.2013.11.2.85
16. I. Casas, J. Giménez, V. Martí, M. E. Torrero, J. de Pablo, “Kinetic studies of unirradiated UO_2 dissolution under oxidizing conditions in batch and flow experiments,” *Radiochim. Acta*, vol. 66–67, no. s1, pp. 23–28, 1994. https://doi.org/10.1524/ract.1994.6667.s1.23
17. J. de Pablo et al., “The oxidative dissolution mechanism of uranium dioxide. I. The effect of temperature in hydrogen carbonate medium,” *Geochim. et Cosmochim. Acta*, vol. 63, no. 19–20, pp. 3097–3103, 1999. https://doi.org/10.1016/S0016-7037(99)00237-9
18. G. S. Goff et al., “Development of a novel alkaline based process for spent nuclear fuel recycling,” *AIChE Annual Meeting, Nuclear Engineering Division*, Salt Lake City (UT), USA, 2007.
19. T. Suzuki, A. Abdelouas, B. Grambow, T. Mennecart, G. Blondiaux, “Oxidation and dissolution rates of UO_2(s) in carbonate-rich solutions under external alpha irradiation and initially reducing conditions,” *Radiochim. Acta*, vol. 94, no. 9–11, pp. 567–573, 2006. https://doi.org/10.1524/ract.2006.94.9-11.567

20. J. S. Goldik, J. J. Noel, D. W. Shoesmith, "Surface electrochemistry of UO_2 in dilute alkaline hydrogen peroxide solutions: Part II. Effects of carbonate ions," *Electrochim. Acta*, vol. 51, no. 16, pp. 3278–3286, 2006. https://doi.org/10.1016/j.electacta.2005.09.019
21. G. Satonnay et al., "Alpha-radiolysis effects on UO_2 alteration in water," *J. Nucl. Mater.*, vol. 288, no. 1, pp. 11–19, 2001. https://doi.org/10.1016/S0022-3115(00)00714-5
22. K. Walenta, "On studtite and its composition," *Am. Mineral.*, vol. 59, pp. 166–171, 1974.
23. M. Deliens, P. Piret, "Metastudtite, $UO_4{\cdot}2H_2O$, a new mineral from Shinkolobwe, Shaba, Zaire," *Am. Mineral.*, vol. 68, pp. 456–458, 1983.
24. R. J. Finch, R. C. Ewing, "The corrosion of uraninite under oxidizing conditions," *J. Nucl. Mater.*, vol. 190, pp. 133–156, 1992. https://doi.org/10.1016/0022-3115(92)90083-W
25. P. C. Burns, K. A. Hughes, "Studtite, $[(UO_2)(O_2)(H_2O)_2](H_2O)_2$: The first structure of a peroxide mineral," *Am. Mineral.*, vol. 88, no. 7, pp. 1165–1168, 2003. https://doi.org/10.2138/am-2003-0725
26. J. Goldik, H. Nesbitt, J. Noël, D. Shoesmith, "Surface electrochemistry of UO_2 in dilute alkaline hydrogen peroxide solutions," *Electrochim. Acta*, vol. 49, no. 11, pp. 1699–1709, 2004. https://doi.org/10.1016/j.electacta.2003.11.029
27. R. Pehrman, "Oxidative dissolution of spent nuclear fuel under the influence of ionizing radiation: Expansion of elementary reactions from UO_2 to $(U,Pu,FP)O_2$," PhD dissertation, University of Helsinki, Faculty of Science, Department of Chemistry, Helsinki, Finland, 2012. Retrieved from: http://urn.fi/URN:ISBN:978-952-10-8147-7 Retrieved on: Apr. 15, 2022
28. В. К. Марков, А. В. Виноградов, С. В. Елинсон, *Уран, методы его определения*, Москва, Россия: Атомиздат, 1960. (V. K. Markov, E. A. Vernyi, A. V. Vinogradov, *Uranium, methods of its definition*, Moscow, Russia: Atomizdat, 1960.)
29. С. Б. Саввин, *Арсеназо III: Методы фотометрического определения редких и актинидных элементов*, Москва, Россия: Атомиздат, 1966. (S. B. Savvin, *Arsenazo III: Methods for the photometric determination of rare elements and actinides*, Moscow, Russia: Atomizdat, 1966.)
30. *Analytical Spectroscopy Library Volume 10: Separation, preconcentration, and spectrophotometry in inorganic analysis*, Z. Marczenko, M. Balcerzak, Eds., 1st ed., New York (NY), USA: Elsevier Science, 2000.
31. J. A. Ghormley, A. C. Stewart, "Effects of γ-radiation on ice," *J. Am. Chem. Soc.*, vol. 78, no. 13, pp. 2934–2939, 1956. https://doi.org/10.1021/ja01594a004
32. A. I. Vogel, *A textbook of quantitative inorganic analysis*, London, UK: Lowe & Brydone Ltd., 1960.
33. A. Chauhan, P. Chauhan, "Powder XRD Technique and its Applications in Science and Technology," *J. Anal. Bioanal. Tech.*, vol. 5, no. 5, article no. 212, 2014. https://doi.org/10.4172/2155-9872.1000212
34. S. Brunauer, P. H. Emmett, E. Teller, "Adsorption of gases in multimolecular layers," *J. Am. Chem. Soc.*, vol. 60, no. 2, pp. 309–319, 1938. https://doi.org/10.1021/ja01269a023
35. Б. Дельмон, *Кинетика гетерогенных реакций*, Москва, Россия: Мир, 1972. (B. Delmon, *Kinetics of heterogeneous reactions, Moscow*, Russia: Mir, 1972.).
36. H. Y. Sohn, "Fundamentals of the kinetics of heterogeneous reaction systems in extractive metallurgy," in: *Rate Processes of Extractive Metallurgy*, H. Y. Sohn, M. E. Wadsworth, Eds., Boston (MA), USA: Springer, 1979. https://doi.org/10.1007/978-1-4684-9117-3_1
37. J. Janeczek, R. C. Ewing, "Phosphatian coffinite with rare earth elements and Ce-rich françoisite-(Nd) from sandstone beneath a natural fission reactor at Bangombé, Gabon," *Mineral. Mag.*, vol. 60, no. 401, pp. 665–669, 1996. https://doi.org/10.1180/minmag.1996.060.401.14
38. M. Fayek, P. Burns, Y-X. Guo, R. C. Ewing, "Microstructures associated with uraninite alteration," *J. Nucl. Mat.*, vol. 277, no. 2–3, pp. 204–210, 2000. https://doi.org/10.1016/S0022-3115(99)00199-3
39. A. V. Boyarintsev et al., "Reprocessing of simulated voloxidized uranium-oxide SNF in the CARBEX process," *Nucl. Eng. Technol.*, vol. 51, no. 7, pp. 1799–1804, 2019. https://doi.org/10.1016/j.net.2019.05.020
40. C. Hou et al., "Ultrasonic-assisted dissolution of U_3O_8 in carbonate medium," *Nucl. Eng. Technol.*, vol. 55, no. 1, pp. 63–70, 2023. https://doi.org/10.1016/j.net.2022.09.025